Energy-based Real-time Monitoring and Intelligent Evaluation of Fresh Concrete Vibration Quality

C. Bian, N.B. Li, Z.M. Liu
General Institute of Water Resources and Hydropower Planning and Design, Ministry of Water Resources, Beijing, The China

Z.H. Tian
College of Water Conservancy and Hydropower Engineering, Hohai University, Nanjing, The China

ABSTRACT:

The consolidation of concrete is crucial to ensure the long-term strength and durability of concrete structures. Although fresh concrete can be consolidated properly via vibration, the consolidation quality heavily relies on construction workers' experience. In this paper, the vibrated energy for unit volume of fresh concrete (*E*) is employed as monitoring index of concrete vibration quality. Meanwhile, an innovative real-time monitoring system for concrete compactness was developed to collect and calculate the index. Besides, a timely and accurate new method for evaluating concrete consolidation quality based on the E and properties of fresh mixer is also provided and its accuracy and reliability are verified by field experiments. The method can not only avoid errors caused by visually observing concrete surface characteristics, but also effectively overcome the deficiencies that vibration process parameters fail to reveal the consolidation quality directly and the shortage that vibration duration as monitoring index cannot accurately assess concrete compactness variation caused by energy attenuation. In all, the new method can realize a fast and intelligent assessment and feedback by warning information and repairing defects in time to control vibration quality of fresh concrete.

Key words: Real-time monitoring, Intelligent concrete vibration, Quality assessment, Vibration energy

1 INTRODUCTION

Vibration should be done properly to ensure the quality of concrete structural components. An sufficient vibration results in the formation of honeycombs, voids and cold joints in hardened concrete, while an excessive vibration can cause segregation and heterogeneous distribution of aggregates[1,2]. Among vibration methods, internal one is the most commonly used[3-4], that is, a vibrator is inserted into the concrete to work, and its action area is approximately cylinder where concrete is finally compacted. The height of cylinder is vibration depth and its radius is called radius of action. Although the specification for vibration has been enforced in concrete constructions, there is a lack of effective equipment and evaluation methods to monitor the real-time vibration effect. Nowadays the in-situ judgment of the proper vibration duration is highly dependent on the experience of the construction worker, thus it is subjective and arbitrary and will result in irreparable quality defects due to failure of timely handling. Therefore, it is significant to monitor and control the vibration quality in real time way.

In this paper, a new index called the vibrated energy for unit volume of fresh concrete or vibrated energy density (*E*) is built and method of setting threshold value for compactness is created by GA (Genetic Algorithm) as well as prediction model of porosity of hardened concrete by theory of SVM (Support Vector Machine). Based on the above research foundation, real-time visual monitoring technology of the vibration quality is developed, which can effectively reduce quality defects in the concrete casting process and improve hardened performances.

2 CONSTRUCTION OF REAL-TIME MONITORING INDEX

2.1 Velocity of vibrated plain concrete v_p

According to the working condition of concrete vibration, the research assumes that: (1) the effective action length of the vibrator is far larger than its diameter, thus ignoring influence of the end; (2) shear stress is evenly distributed along the axial direction of vibrator; (3) fresh mixture within the vibrated area is sheared and thinned, and is regarded as an isotropic stable uniform incompressible viscous fluid with only radial flow, then the fluid continuity equation is:

$$\frac{1}{r}\times\frac{\partial}{\partial r}\left(rv_p\right)=0 \tag{1}$$

According to the wall boundary condition, when $r=R_0$ (radius of the vibrator), then $v_p=\beta v_{max}=2\pi\beta fA$, where β is the damping coefficient , representing the attenuation of vibrating speed of vibrator after it is inserted into concrete, and its value is obtained from tests; while r =∞ , $v_p=0$, thus the condition is substituted into Eq. (1) , it is shown as:

$$v_p=2\pi\beta fA\left(\frac{R_0}{r}\right)^2 \tag{2}$$

where r = the shortest distance from rod axis, m; f = frequency of rod, Hz; A = amplitude, m. It is said that the fresh vibrated concrete behaves as power-law fluid[1,2], thus:

$$\tau_{ij}=K\left(\frac{1}{2}\dot{I}_2\right)^{\frac{n-1}{2}}A_{ij} \tag{3}$$

where A_{ij} = first order Rivilin-Ericksen tensor; K = consistency coefficient; n = flow index; $\dot{I}_2$ = the second invariant of strain rate tensor whose expression is:

$$\dot{I}_2=A_{rr}^2+A_{\theta\theta}^2=4\left(\frac{\partial v_p}{\partial r}\right)^2+4\frac{v_p^2}{r^2} \tag{4}$$

From Mises yield criterion, the expression of shear yield strength K_y is:

$$K_y=\frac{1}{\sqrt{6}}\sqrt{\left(\tau_{rr}-\tau_{\theta\theta}\right)^2+\left(\tau_{rr}-\tau_{zz}\right)^2+\left(\tau_{\theta\theta}-\tau_{zz}\right)^2}=\frac{\sqrt{210}}{15}\times10^{\frac{n}{2}}\mathrm{K}\left(2\pi\beta fAR_0^2\frac{1}{r^3}\right)^n \tag{5}$$

According to Spangenberg et al., when K_y is greater than τ_0 , concrete will flow[3]. From Eq. (5), K_y decreases gradually with increasing value of r, and when it decreases to the yield stress τ_0 at the boundary of action range, thus the action radius of rod is expressed as:

$$R_{is}=10^{\frac{1}{6}}\left(2\pi\beta fAR_0^2\right)^{\frac{1}{3}}\left(\frac{\sqrt{210}K}{15\tau_0}\right)^{\frac{1}{3n}} \tag{6}$$

2.2 Velocity of vibrated reinforced concrete v_s

When the rod vibrates in reinforced concrete, steel layers are regarded as porous medium, i.e., equal-diameter parallel capillary tubes whose thickness of wall is diameter of the bar, diameter of the tube is clear distance between adjacent bars. Besides, spatial variation of concrete velocity from vibrator to reinforcement is ignored, then flow of vibrated fresh mixture within steels is regarded as seepage of porous media[4]. In other words, the flow is assumed as stable radial laminar flow and its behavior follows Darcy's law of permeability, the velocity expression is:

$$v_s=-\frac{k}{\mu_{app}}\frac{dP}{dr} \tag{7}$$

where k = permeability coefficient, m^2; $\frac{dP}{dr}$ = the fluid pressure gradient along the radial direction, Pa / m; μ_{app} = the apparent viscosity of vibrated mixture, Pa.s, which is expressed as:

$$\mu_{app} = \frac{\tau}{\dot{\gamma}} = \frac{K\dot{\gamma}^n}{\dot{\gamma}} = K\dot{\gamma}^{n-1} \tag{8}$$

According to Perrin et al[5], the shear rate of non-Newtonian fluid flow within porous mediums similar to reinforced layers is expressed as:

$$\dot{\gamma} = \frac{\alpha \times v_s}{\sqrt{k \times \phi}} \tag{9}$$

where ϕ =porosity; α = shape factor, value between 1-5.2[6].Jointing Eq. (8), (9) and (10), it can be obtained as follows:

$$v_s = \left(\frac{-k^{\frac{n+1}{2}} \phi^{\frac{n-1}{2}}}{K\alpha^{n-1}} \frac{dP}{dr} \right)^{\frac{1}{n}} \tag{10}$$

In the place where $r = R_0$, due to blocking and attenuation of vibration energy from steels, the shear rate at the interface between rod body and concrete increases, and slip occurs there[7]. Considering complex mechanism of boundary slip resulting in great difficulty of theoretically deriving boundary velocity v_0, the v_0 is derived by dimensional analysis. Since v_0 is influenced by f, A, k, ϕ, α, τ_0 and μ, it is expressed as:

$$v_0 = \delta\alpha (fA)^{\frac{3}{4}} (k\phi)^{\frac{1}{8}} \left(\frac{\tau_0}{\mu} \right)^{\frac{1}{4}} \tag{11}$$

Besides, when $r=\infty$, $v_s=0$, thus v_s is expressed as:

$$v_s = \frac{\delta\alpha (fA)^{\frac{3}{4}} (k\phi)^{\frac{1}{8}} \left(\frac{\tau_0}{\mu} \right)^{\frac{1}{4}} R_0}{r} \tag{12}$$

The molecular expression in Eq. (12) is denoted by B. From Mises yield criterion, K_y is shown as:

$$K_y = \frac{1}{\sqrt{6}} \sqrt{(\tau_{rr} - \tau_{\theta\theta})^2 + (\tau_{rr} - \tau_{zz})^2 + (\tau_{\theta\theta} - \tau_{zz})^2} = K \left(\frac{2B}{r^2} \right)^n \tag{13}$$

Thus when the vibrator is inserted into reinforced concrete, the action radius R_{is}^s is shown as:

$$R_{is}^s = \sqrt{2\alpha\delta R_0} (fA)^{\frac{3}{8}} \left(\frac{\tau_0}{\mu} \right)^{\frac{1}{16}} (k\phi)^{\frac{1}{16}} \left(\frac{K}{\tau_0} \right)^{\frac{1}{2n}} \tag{14}$$

According to Vasilic's research[8], k consists of k_{pe} whose permeability direction is vertical to the main steels and k_{pa} whose direction is parallel to those, in addition, $k_{pa}=2k_{pe}$, k_{pe} is shown as [9]:

$$k_{pe} = -\frac{(M_{sm} + d_{sm})}{16} \left[2\ln(y) + (1-y)^2 / (1+y)^2 + (1-y^4) / 2(1+y^4) \right] \tag{15}$$

where M_{sm} and d_{sm} are clear distance between adjacent main steels and diameter of the steels respectively, m. Thus:

$$\alpha k^{\frac{1}{8}} = \sqrt{\alpha_{pe}^2 k_{pe}^{\frac{1}{4}} + \alpha_{pa}^2 k_{pa}^{\frac{1}{4}}} \tag{16}$$

where $\alpha_{pa}=2\alpha_{pe}$. In this paper, $\alpha_{pe}=1$, thus:

$$\alpha k^{\frac{1}{8}}=\sqrt{4\sqrt{2}+1}k_{pe}^{\frac{1}{8}}\approx 2.58k_{pe}^{\frac{1}{8}} \tag{17}$$

In addition to main steels, transverse ones such as distributed reinforcement and stirrup are also arranged, resulting in reduction of permeability and flow speed[8].It is assumed the permeability coefficient k *is* linearly proportional to the relative distance x which equals M_{ss} divided by d_{ss}, and M_{ss} is clear distance between adjacent transverse steel while d_{ss} is the diameter of transverse one. Jointing Eq. (12), (15) -(18), it can be obtained as follows:

$$\begin{cases} v_s=\dfrac{2.58\delta(fA)^{\frac{3}{4}}\left(k_{pe}\psi\dfrac{M_{ss}}{d_{ss}}\phi\right)^{\frac{1}{8}}\left(\dfrac{\tau_0}{\mu}\right)^{\frac{1}{4}}R_0}{r} \\ R_{is}^{s}=\sqrt{2\alpha\delta R_0}(fA)^{\frac{3}{8}}\left(\dfrac{\tau_0}{\mu}\right)^{\frac{1}{8}}\left(k_{pe}\psi\dfrac{M_{ss}}{d_{ss}}\phi\right)^{\frac{1}{16}}\left(\dfrac{K}{\tau_0}\right)^{\frac{1}{2n}} \\ k_{pe}=-\dfrac{(M_{sm}+d_{sm})}{16}\left[2\ln(y)+(1-y)^2/(1+y)^2+(1-y^4)/2(1+y^4)\right] \end{cases} \tag{18}$$

where ψ is attenuation coefficient of permeability after arranging transverse steels. Values of ψ and δ are obtained from tests.

2.3 Determination of empirical parameters β, δ and ψ

The action radius is measured by the method recommended by French Concrete Association [10].Fresh concrete was prepared based on the mixture design of the construction. A bucket cylinder with a diameter of 50 cm and a depth of 30 cm was used to cast fresh concrete and foam rubbers are pasted on the bottom and surface to eliminate energy reflection. The vibrators with ϕ 25 mm and ϕ 35 mm were held by a tripod and immersed individually into the bucket cylinder to vibrate and consolidate the concrete (Figure 1a). A series of markers were placed on the surface of the fresh concrete with a space interval of 1 cm, as shown in Figure 1b and 1c. After vibration, the markers were completely submerged in the fresh concrete within the liquid region, indicating the radius of action, as shown in Fig. 1b and 1d. Meanwhile, the frequency and amplitude of rod are measured respectively when it vibrates in air and within concrete. The rheological parameters of concrete are measured by self-made rheometer.

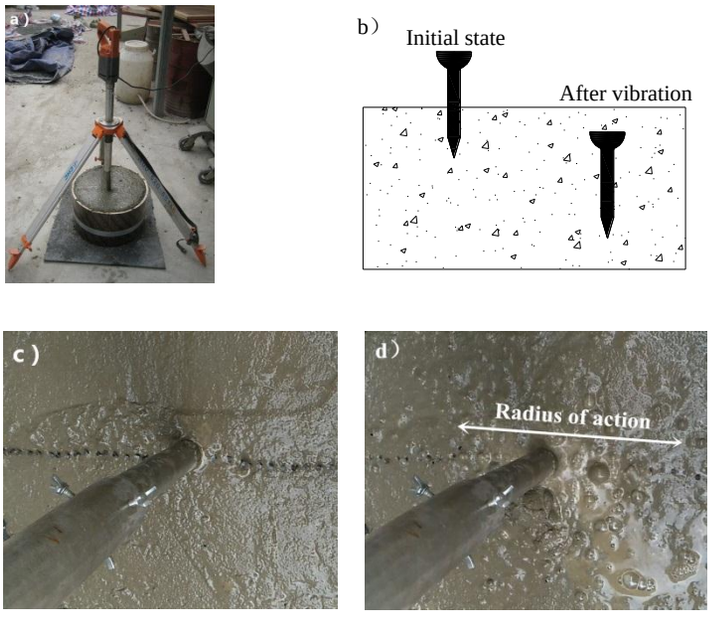

Figure 1. The radius of action measurement: a) experiment setup; b) the marker on the fresh concrete surface; c) before vibration; d) after vibration.

The mixture proportions are listed in Table 1, among them, Mix R-C2 is adopted in tests of reinforced concrete with vibrator of ϕ 35 mm and the steel arrangements are listed in Table 2 where $x_{sm} = M_{sm}/d_{sm}$.

Table 1. The mix proportion of concrete in tests of action radius.

Number	W/C	Paste-aggregate ratio	Sand ratio (%)	Cement quantity (kg/m^3)	SP content (%)	Thickener content (%)
R-C1	0.55	0.64	45	340	0.4	0
R-C2	0.50	0.64	43	315	0.4	0
R-C3	0.45	0.64	43	353	0.1	0.03
R-C4	0.45	0.64	43	381	0.1	0.02
R-C5	0.40	0.64	48	403	0.1	0.05
R-C6	0.40	0.64	48	420	0.1	0.05

Table 2. Scheme of steels arrangement.

Number	Main steels (mm)	Tranverse steels (mm)	x_{sm}	x_{ss}
S1	10@100	10@200	9.0	19.0
S2	10@100	8@100	9.0	11.5
S3	10@100	10@100	9.0	9.0
S4	12@100	10@100	7.3	9.0
S5	14@100	10@100	6.1	9.0

Test results show that when the vibrator is inserted into the concrete, its frequency and amplitude will decrease, and are mainly affected by plastic viscosity. The decreasing ranges with the viscosity follow power-law function individually and correlation coefficient is about 0.98. The fitting formula is shown as:

$$\frac{\Delta f}{f}\times 100\% = 2.53\mu^{0.37} \tag{19}$$

$$\frac{\Delta A}{A}\times 100\% = 0.63\mu^{0.47} \tag{20}$$

Thus β is expressed as:

$$\beta = \left(1-\frac{\Delta f}{f}\right)\cdot\left(1-\frac{\Delta A}{A}\right) \approx \left(1\text{-}0.03\mu^{0.37}\right)\left(1\text{-}0.01\mu^{0.47}\right) \tag{21}$$

Substituting Eq. (21) into Eq. (6), and $\delta \approx 5.27$, $\psi \approx 0.07$ is obtained by fitting Eq. (6) and (18) with the measured value of action radius. The prediction results are shown in Figure 2 and 3.

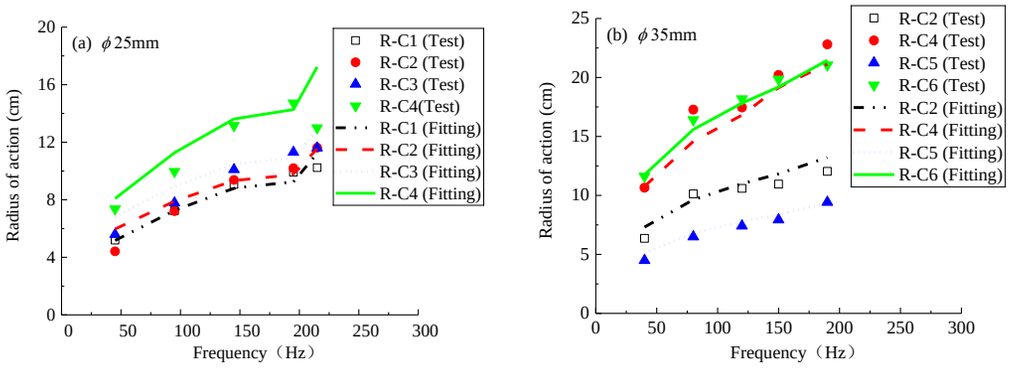

Figure 2. Prediction results of action radius of vibrator in plain concrete.

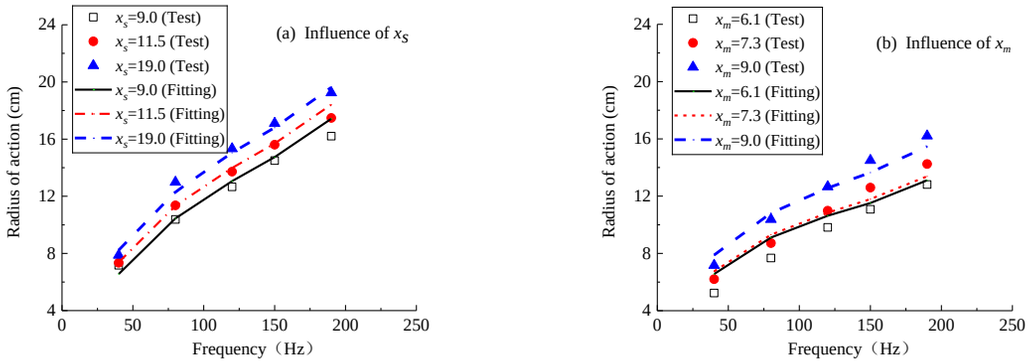

Figure 3. Prediction results of action radius of vibrator in reinforced concrete.

Except for condition of lower vibrating intensity, the predicting accuracy of action radius under other conditions is relatively higher. The empirical coefficients and the prediction equations of action radius are feasible to guide concrete casting on site allowing for high fluidity of concrete and vibrating energy, therefore the action radius of vibrator inserted in plain and reinforced concrete are expressed respectively as:

$$R_{is}=2.71\left[\left(1\text{-}0.03\mu^{0.37}\right)\left(1\text{-}0.01\mu^{0.47}\right)fAR_0^2\right]^{\frac{1}{3}}\left(\frac{\sqrt{210K}}{15\tau_0}\right)^{\frac{1}{3n}} \tag{22}$$

$$\begin{cases} R_{is}^{s}=4.42R_0^{\frac{1}{2}}\left(fA\right)^{\frac{3}{8}}\left(\dfrac{\tau_0}{\mu}\right)^{\frac{1}{8}}\left(k_{pe}\psi\dfrac{M_{ss}}{d_{ss}}\phi\right)^{\frac{1}{16}}\left(\dfrac{K}{\tau_0}\right)^{\frac{1}{2n}} \\ k_{pe}=-\dfrac{\left(M_{\mathrm{sm}}+d_{\mathrm{sm}}\right)}{16}\left[2\ln\left(y\right)+\left(1-y\right)^2/\left(1+y\right)^2+\left(1-y^4\right)/2\left(1+y^4\right)\right] \end{cases} \tag{23}$$

2.4 Vibrated energy density of fresh concrete E

According to Kirham's energy equation[11], the vibrated energy density of fresh concrete is expressed as:

$$E=\rho t\frac{v^2}{4\pi^2}f \tag{24}$$

where ρ = density of fresh concrete, kg / m^3; t =vibration time, s; f =vibration frequency, Hz; v = flow speed of fresh mixture at the distance R from rod axis, m/s. Substituting Eq.(2), (18) and (21) and empirical coefficients into Eq.(24), and energy density of plain concrete E_p and that of steel concrete E_s are shown as:

$$\begin{cases} E_p=\rho tf^3\left[\left(1\text{-}0.03\mu^{0.37}\right)\left(1\text{-}0.01\mu^{0.47}\right)A\right]^2\left(\dfrac{\mathrm{R}_0}{r}\right)^4 \\ E_s=2.42\rho tf^{\frac{5}{2}}A^{\frac{3}{2}}\left(k_{pe}\dfrac{M_{ss}}{d_{ss}}\phi\right)^{\frac{1}{4}}\left(\dfrac{\tau_0}{\mu}\right)^{\frac{1}{2}}\left(\dfrac{\mathrm{R}_0}{r}\right)^2 \\ k_{pe}=-\dfrac{\left(M_{\mathrm{sm}}+d_{\mathrm{sm}}\right)}{16}\left[2\ln\left(y\right)+\left(1-y\right)^2/\left(1+y\right)^2+\left(1-y^4\right)/2\left(1+y^4\right)\right] \end{cases} \tag{25}$$

3 RAPID EVALUATION METHOD OF VIBRATION QUALITY BASED ON *E*

Through a large number of experiments by measuring the cored porosity of hardened concrete p at different distances from vibrating source, and then based on theory of support vector machine (SVM), statistical prediction model of the porosity p influenced by characteristics of fresh mixture and the vibration energy density of concrete is established. Finally, the minimum porosity $p_{\min}$ and corresponding threshold value of the energy density E_0 when concrete is compacted well are determined by genetic algorithm (GA) .

3.1 Prediction model of porosity for hardened concrete

A total of 100 sets of data were collected in which trained group includes 85 sets numbered #1-85 while tested one includes 15 sets numbered #86-100. Input and output parameters are shown in Table 3 and E is calculated by Eq. (25). The kernel function employs Gaussian radial basis function (RBF). The model parameters include insensitive loss function, penalty factor c and width parameter g of RBF, where values of c and g are at discretion. Method of 5-fold cross validation is used to avoid over learning, and optimal values of c and g are 5.6569 and 2.8284 respectively.

Table 3 Input and output parameters.

Input parameters	Out parameters
Air content, τ_0, μ, ρ, E	p

Prediction results are shown in Figure 4 and mean square error (MSE) equals 0.02879. The predicted values of porosity fit well with measured ones. Except for individual points, the relative error is less than 10%, indicating the porosity can be rather accurately predicted by method of SVM.

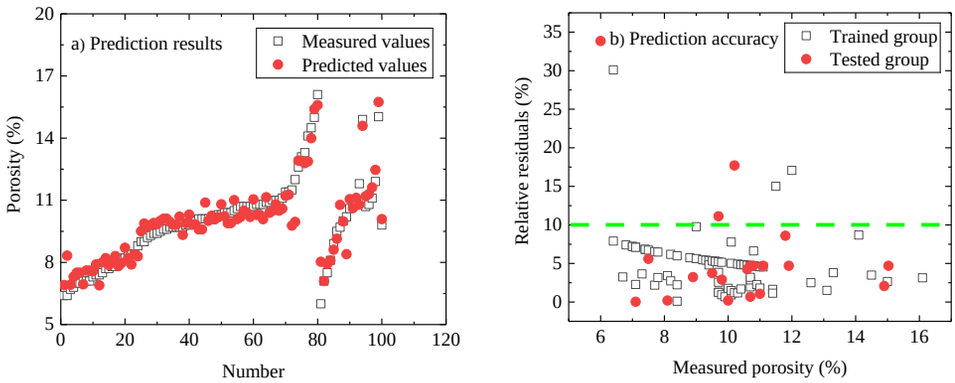

Figure 4. Prediction results of modeling by SVM.

3.2 Inverse analysis for the threshold value E_0

After modeling of porosity by SVM, for typical concrete, values of input parameters involved in fresh mixture performances in the model are kept unchanged and predicted values of porosity are calculated by varied E. Then input parameters of SVM and concrete porosity are taken as population individuals and individual fitness degree respectively. The number of iterations and individuals are 100 and 20 individually, the probability of crossover and variation are 0.4 and 0.2 respectively and individual length is 5.

3.3 Real-time evaluation model of concrete compactness

The real-time evaluation model will determine compaction state of meshed voxels in the casting area and graphically displayed. The voxel compactness is determined by:

$$\begin{cases} E_v = E_0 V_v \\ \left|\dfrac{E_r - E_v}{E_v}\right| \le \delta \quad \text{Compactness} \\ -2\delta \le \dfrac{E_r - E_v}{E_v} < -\delta \quad \text{First-degree inadequate vibration} \\ \dfrac{E_r - E_v}{E_v} < -2\delta \quad \text{Second-degree inadequate vibration} \\ \delta < \dfrac{E_r - E_v}{E_v} \le 2\delta \quad \text{First-degree excessive vibration} \\ \dfrac{E_r - E_v}{E_v} > 2\delta \quad \text{Second-degree excessive vibration} \end{cases} \tag{26}$$

where V_v = real volume of fresh concrete represented by single voxel, m^3; E_v = threshold value of energy for compacted voxel, J; δ = tolerance rate of the energy and the default is 0.2 usually according to construction quality requirements; E_r =vibrated energy for volume of concrete V_v, J. The E_r is expressed as:

$$E_r = \sum_{i=1}^{T} E_i \tag{27}$$

where $T = \dfrac{t}{\Delta t}$, Δt = the period for real-time collecting vibration points data and the default is 1 second. For plain concrete, the E_i is shown as:

$$\begin{cases} r_i > R_{is}, E_i = 0, \ i=1,2\cdots T \\ r_i \le R_{is}, E_i = \rho \Delta t V_v f^3 \left[\left(1\text{-}0.03\mu^{0.37}\right)\left(1\text{-}0.01\mu^{0.47}\right)A\right]^2 \left(\dfrac{R_0}{r_i}\right)^4 \end{cases} \tag{28}$$

where R_{is} = calculated from Eq.(23), m; r_i = distance from the voxel i to rod axis, m. While for reinforced concrete, the E_i is shown as:

$$\begin{cases} r_i > R_{is}^s, E_i = 0, \ i=1,2\cdots T \\ r_i \le R_{is}^s, E_i = 2.42\rho \Delta t f^{\frac{5}{2}} A^{\frac{3}{2}} V_v \left(k_{pe}\dfrac{M_{ss}}{d_{ss}}\phi\right)^{\frac{1}{4}} \left(\dfrac{\tau_0}{\mu}\right)^{\frac{1}{2}} \left(\dfrac{R_0}{r_i}\right)^2 \\ k_{pe} = -\dfrac{\left(M_{sm}+d_{sm}\right)}{16}\left[2\ln(y) + (1-y)^2/(1+y)^2 + \left(1-y^4\right)/2\left(1+y^4\right)\right] \end{cases} \tag{29}$$

4 REAL-TIME MONITORING OF CONCRETE VIBRATION QUALITY

In order to realize monitoring of the energy density E, the original real-time visual monitoring system for vibration effects on fresh concrete has been updated by supplementing new parameters such as τ_0, μ, d_{sm} and so on into analysis[12]. The system consists of moving stations including vibrators, positioning base station, cloud server and controlling center, as shown in Figure 5.The related information of vibration quality is collected by intelligent wearable monitoring equipment and transmitted by WiFi or GPRS network to cloud server. Then software of the clients in the controlling center downloads the information and analyses, finally displaying the quality and feedback warnings of defective areas to site for re-vibration to improve performances of concrete structure. In the Figure 5b, defective sections are marked by red line box. Besides, the under, over, and normally vibrated areas are displayed in red/yellow, cyan and green colors.

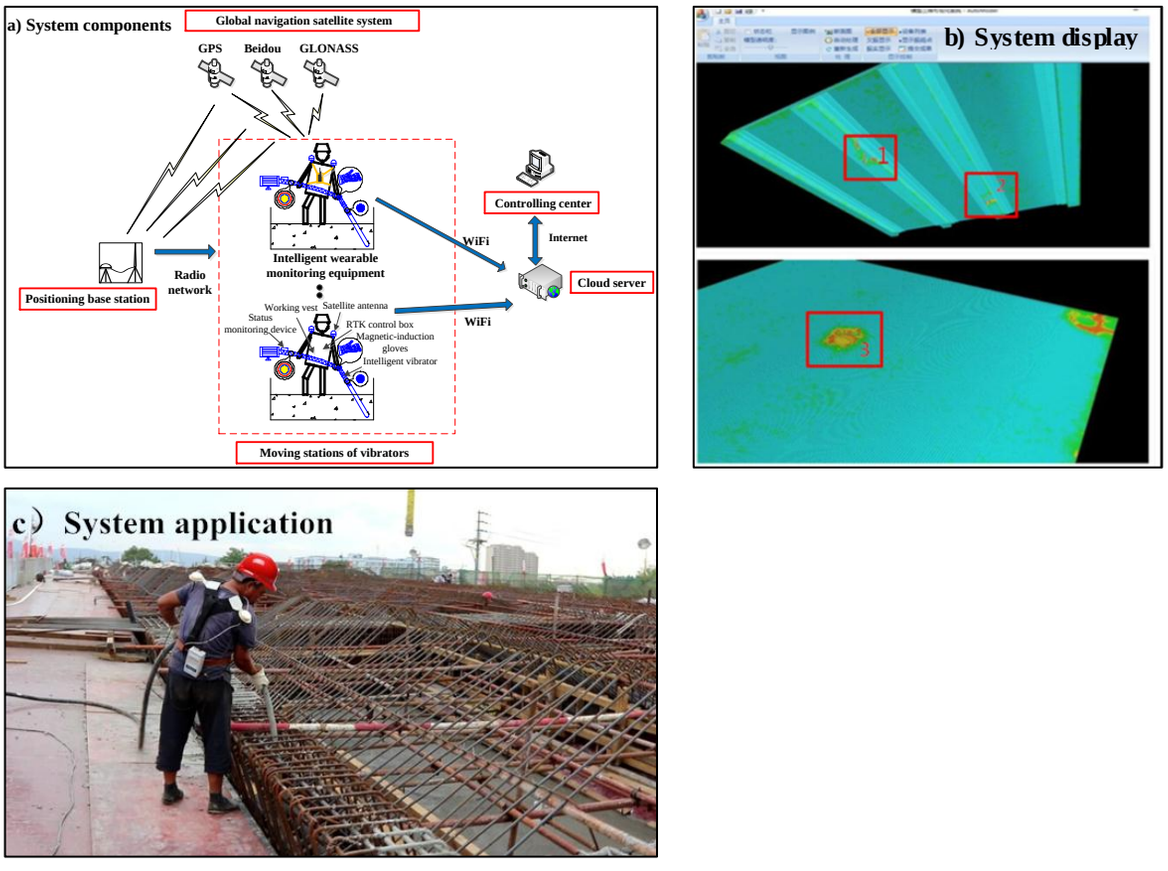

Figure 5. Framework of visual monitoring system of vibration effect.

5 ON-SITE CASE STUDY TO EVALUATE THE RELIABILITY OF THE SYSTEM

The system has been applied to casting of baseplates of section 6-8 in the assembly bay of Guanyinyan hydropower house in China, and 4 sets of equipments have been put into use on site. The reinforcement is arranged in the way of two-way double row slab, the distribution of reinforced bars is Φ 16mm@150mm while that of distributing bars is Φ 10mm@150mm, the steel ratio is 0.34%. the w/c ratio of concrete is 0.4 and sand rate is 42%, mixing continuous crushed stone with d_{max} of 30mm and polycarboxylate superplasticizer with content of 0.6%. The action of radius is 18cm (about 3.6 times of rod diameter) and the threshold value of energy density is about 140.6 J/m^3.

In order to validate reliability of the system, the quality of displayed defective area will be verified by nondestructive impact-echo method (IES)[13]. The results tested by IES and the system are shown in Table 4

Table 4. Comparison of inadequate vibrated areas measured by the system and the IES method.

Locations	Areas measured by the system (m^2)	Areas measured by the IES method (m^2)	Relative errors (%)
Section 6th 1#	2.94	3.29	10.60
Section 6th 2#	0.97	1.07	9.30
Section 7th 1#	2.77	2.91	4.80
Section 7th 2#	2.48	2.76	10.10
Section 7th 3#	1.93	2.18	11.50
Section 8th	3.55	3.91	9.20

The inadequately vibrated area calculated by the system and IES method respectively only has an average relative error of no more than 10%, indicating accuracy and reliability of the system can satisfy construction requirements in consideration of difficult quality control for concrete casting on site due to influences of complex construction conditions. After visualization, the information of defects is sent promptly to the construction inspector and the defects can be easily removed by conducting a re-vibration process to ensure hardened performances of concrete structure.

6 CONCLUSIONS

(1) In this paper, vibrated energy density of fresh concrete is established and then prediction model of porosity of hardened concrete is also created, thus obtaining minimum porosity and threshold value of the energy density for certain concrete mix. Test results show that the porosity is predicted well and the threshold has a rather high accuracy.

(2) Based on real-time evaluation model of concrete compactness, the updated real-time visual monitoring system including developed intelligent wearable equipment is reliable and accurate to graphically display and feedback vibration quality.

(3) Following studies will focus on improving predictive accuracy for porosity by increasing amount and representativeness of tested data. Meanwhile broadening application range of the system by developing other positioning technologies such as ultra wide band (UWB) will be researched as well as corresponding study of data analysis and mining.

ACKNOWLEDGEMENTS

This study is financially supported by National Key Research and Development Project of China (2016YFC0401805; 2017YFC0404805), and supported by National Natural Science Foundation of China (No. 51879094).

REFERENCES

[1] Tattersall, G. H. & Baker, P. H. 1989. Investigation on the effect of vibration on the workability of fresh concrete using a vertical pipe apparatus. *Magazine of Concrete Research* 41(146): 3-9.

[2] Pichler, C., Röck, R. & Lackner, R. 2017. Apparent power-law fluid behavior of vibrated fresh concrete: Engineering arguments based on Stokes-type sphere viscometer measurements. *Journal of Non-Newtonian Fluid Mechanics* 240:44-55.

[3] Spangenberg, J., Roussel, N., Hattel, J. H., et al. 2012. Flow induced particle migration in fresh concrete: Theoretical frame, numerical simulations and experimental results on model fluids. *Cement and Concrete Research* 42(4): 633-641.

[4] Vasilic, K., Meng, B., Kühne, H. C., et al. 2011. Flow of fresh concrete through steel bars: A porous medium analogy. *Cement and Concrete Research* 41(5): 496-503.

[5] Perrin, C. L., Tardy, P. M., Sorbie, K. S., et al. 2006. Experimental and modeling study of Newtonian and non-Newtonian fluid flow in pore network micromodels. *Journal of Colloid and Interface Science* 295(2): 542-550.

[6] Lopez, X., Valvatne, P. H. & Blunt, M. J. 2003. Predictive network modeling of single-phase non-Newtonian flow in porous media. *Journal of Colloid and Interface Science* 264(1): 256-265.

[7] Wu, C. W., Ma, G. J., Zhou, P. 2008. A review of the study on the boundary slip problems of fluid flow. *Advances in Mechanics* 38(3): 265-282 (in Chinese).

[8] Ksenija, V. 2016. A Numerical model for self-compacting concrete flow through reinforced sections: A porous medium analogy. *Federal Institute for Material Testing*. Germany.

[9] Boutin, C. 2000. Study of permeability by periodic and self-consistent homogenization. *European Journal of Mechanics - A/Solids* 19(4): 603-632.

[10] Grampeix, G. & Dupoirier, N. R. J. 2013. Internal vibration and viscous concrete: application and prediction of the radius of action. In Roussel, N. & Bey, H. B. (ed.), *Rheology and Processing of Construction Materials - 7th RILGM International Conference on Self-Compacting Concrete and 1st RILGM International Conference on Rheology and Processing of Construction Materials*. France: Paris.

[11] Kirkham, R. H. H. & Whiffin A. C. 2015. The compaction of concrete slabs by surface vibration: first series of experiments. *Magazine of Concrete Research* 3(8):79-91.

[12] Tian, Z. H., Sun, X., Su, W. H., et al. 2019. Development of real-time visual monitoring system for vibration effects on fresh concrete. *Automation in Construction* 98: 61-71.

[13] Zhang, M. & Zhang Y. 2016. Study on the internal defects of concrete slab on the basis of IES. *International Conference on Civil, Transportation and Environment*. China: Guangzhou.